Analysis of Unsteady Aerodynamics for Elastic Bodies in Supersonic Flow

Pablo Garcia-Fogeda* and D. D. Liu†
Arizona State University, Tempe, Arizona

The harmonic potential panel method (HPP, also known as HGM) developed for nonplanar wings in supersonic flight is generalized in its capability to include flexible bodies performing bending oscillations. Three different coordinate systems (namely, the wind-fixed, body-fixed, and pseudo-wind-fixed) are first investigated. It is shown that the singularity at the apex is removed in the last two coordinate systems. The present HPP method is based on the formulation of a line-doublet paneling scheme, which is general for axisymmetric bodies of arbitrary shapes, allows for slope discontinuity, and is valid in the full frequency range. Because of the harmonic gradient model, the number of elements required is least affected by the given Mach number and reduced frequency. To validate the present HPP method, the computed results in various limits are verified with slender-body theory, piston theory, measured stability derivatives, and steady velocities, as calculated by other methods for different body shapes.

Nomenclature

C_p^0 = mean pressure coefficient
C_p^1 = unsteady pressure coefficient
$g(x)$ = normalized natural mode shape
k = reduced frequency, $\omega L/U_\infty$
L = body length
M_∞ = freestream Mach number
t = time in a coordinate system moving relative to freestream
U_∞ = freestream velocity
x,r,θ = cylindrical coordinates
x_G = center of oscillation
β = $\sqrt{M_\infty^2-1}$
γ = ratio of specific heats
δ_0 = amplitude of normal coordinate
ξ = dipole coordinate
ϕ_0 = mean perturbed potential
ϕ_1 = unsteady perturbed potential
τ = time in wind-fixed system
ω = circular frequency
Ω = full velocity potential

$$\square = -\beta^2\frac{\partial^2}{\partial x^2}+\frac{\partial^2}{\partial r^2}+\frac{1}{r}\frac{\partial}{\partial r}$$

Subscripts

x,r,θ,t,τ = partial derivatives

Introduction

WHEN cruising at supersonic speeds, slender-body/wing configurations are susceptible to a number of aeroelastic instabilities. It is known that the stability and control characteristics of high-speed flexible bodies may be significantly influenced by the distortion of the structure under transient loading conditions. Also, the problem of store/airframe interaction during the cruise and/or maneuver phase of modern aircraft has been a major concern for design and performance. The effects of this type of interaction could sometimes change the air load and hence the wing flutter characteristics rather drastically. For example, problems such as stores in pitch-yaw combined oscillations and the tip-missile influence are among the critical factors related to aircraft flutter. Clearly, the prediction of these boundaries relies almost exclusively on the unsteady aerodynamic inputs. The objective of the present work is, therefore, to provide a generalized harmonic potential panel (HPP) method for computing the unsteady aerodynamics of arbitrary flexible bodies in the supersonic flow regime.

Currently, several panel methods have claimed success for predictions of the steady aerodynamics for wing/body combinations in the supersonic flow regime (see, e.g., Refs. 1 and 2). In recent years, computational methods for unsteady supersonic flow prediction have been investigated by many (e.g., Ref. 3). However, these approaches are usually formulated for wing planform calculations. On the other hand, the investigation of unsteady supersonic flow for oscillating bodies in the past has usually been based on slender- or not-so-slender-body theories for rigid-body oscillations in the low-frequency range.[4-11] It appears that little progress has been made in the development of a viable computational method for wing-body or body-fin combinations for unsteady supersonic aerodynamic predictions that is uniformly valid in the complete frequency domain.

In the present development, the harmonic potential panel (HPP) method for unsteady aerodynamic predictions of multiple, nonplanar wings is extended to include a computational procedure for axisymmetric bodies.

Special emphasis has been placed on the proper choice of a suitable coordinate system. For bodies in pitch motion, the coordinate system in question has been subject to some controversy in the past.[8] Three systems are identified in our analysis: wind-fixed, body-fixed, and pseudo-wind-fixed. When the wind-fixed system is applied in a straightforward manner, it is found that the solution obtained is totally contaminated by a spurious leading-edge singularity. Such singularities are absent or can be removed in the latter two systems; consequently, approximated solutions obtained yield results in favorable agreements with each other.

Because the present HPP method is based on the formula-

Presented as Paper 86-0007 at the AIAA 24th Aerospace Sciences Meeting, Reno, NV, Jan. 6-9, 1986; received Sept. 16, 1986; revision received March 16, 1987.

*Faculty Associate, Department of Mechanical and Aerospace Engineering. Member AIAA.
†Associate Professor, Department of Mechanical and Aerospace Engineering. Member AIAA.

tion of a line-doublet paneling scheme, it is completely general for axisymmetric bodies of arbitrary shapes allowing for slope discontinuities and is valid in the full frequency range. In fact, the HPP method normally requires as few as 40 panels. Similar to the HPP computation for wings, the panel number required here is least affected by the given Mach number and the frequency variations. To validate the present method, computed results in various limits are verified with slender-body theory, piston theory, computed steady pressures, and measured stability derivatives.

Formulation

Following Miles'[12] treatment of pointed slender bodies in supersonic flow, one begins with the full potential equation,

$$a^2\nabla^2\Omega=\Omega_{\tau\tau}+\frac{\partial}{\partial\tau}(\nabla\Omega)^2+\frac{1}{2}(\nabla\Omega\cdot\nabla)(\nabla\Omega)^2 \tag{1}$$

where a is the local speed of sound given by

$$a^2=(1/M_\infty^2)-(\gamma-1)\{\Omega_\tau+\tfrac{1}{2}[(\nabla\Omega)^2-1]\} \tag{2}$$

The time coordinate above is based on a spatial coordinate system that is fixed with respect to the fluid at infinity.

It is known that various linearized small-disturbance equations can be derived from Eq. (1), depending on the coordinate system chosen.[13] Their formulations according to the wind-fixed, body-fixed, and pseudo-wind-fixed coordinate systems are discussed in order.

Wind-Fixed Coordinates

If a coordinate system parallel to the freestream velocity is adopted for the small-disturbance flow, then the full potential Ω can be written as

$$\Omega(x,r,\theta,\tau)=x+\phi_0(x,r)+\delta_0\phi_1(x,r)e^{ik\tau}\cos\theta \tag{3}$$

The linearized equations for ϕ_0 and ϕ_1 are obtained, i.e.,

$$\Box\phi_\sigma=\sigma\cdot\left\{\left[2ikM_\infty^2\phi_{\sigma_x}+\left(\frac{1}{r^2}-M_\infty^2k^2\right)\phi_\sigma\right]+G_0\right\} \tag{4}$$

with $\sigma=0$ for ϕ_0 and $\sigma=1$ for ϕ_1, respectively defining Eqs. (4a) and (4b). By letting $G_0=0$ in Eq. (4), we define Eq. (4) as the governing equation in the wind-fixed system. The initial data are provided by the Mach wave conditions at the body apex,

$$\phi_\sigma=\phi_{\sigma_x}=\phi_{\sigma_r}=0 \qquad \text{for } x-\beta r\le 0 \tag{5}$$

The instantaneous position of the body is specified by

$$r=R(x)-\delta_0e^{ik\tau}g(x)\cos\theta \tag{6}$$

The boundary conditions at the body surface after Taylor expansion with respect to the body mean position reads, at $r=R(x)$,

$$\phi_{\sigma_r}-R'(x)\phi_{\sigma_x}=(1-\sigma)R'(x)+\sigma\cdot[-g'(x)-ikg(x)+B_0(g,\phi_0)] \tag{7}$$

where

$$B_0(g,\phi_0)=g(x)(\phi_{0rr}-R'\phi_{0xr})-g'(x)\phi_{0x}$$

The exact isentropic pressure coefficient is expanded to yield the mean flow and unsteady flow pressure coefficients,

$$C_p=C_p^0+C_p^1\delta_0e^{ik\tau}\cos\theta$$

$$C_p^0=\frac{2}{\gamma M_\infty^2}[S_0^\gamma-1]$$

$$C_p^1=-2S_0\cdot\{[(1+\phi_{0x})\phi_{1x}+\phi_{0r}\phi_{1r}+ik\phi_1]+J_0(g,\phi_0)\} \tag{8}$$

where

$$S_0=\left[1-\frac{\gamma-1}{2}M_\infty^2(2\phi_{0x}+\phi^2{}_{0x}+\phi_{0r}^2)\right)^{1/(\gamma-1)} \tag{9}$$

$$J_0(g,\phi_0)=-g(x)[\phi_{0xr}(1+\phi_{0x})+\phi_{0rr}\phi_{0r}] \tag{10}$$

Clearly, the second-order derivative terms in Eqs. (7) and (10) associated with $g(x)$ will result in an apex singularity if $g(0)$ does not vanish. For example, in the case of slender-body approximation, the term $g(x)\phi_{0rr}$ behaves like $1/x$ for a nonvanishing $g(x)$ at the apex. The cause of this apex singularity was discussed by Platzer and Liu,[14] where they pointed out that it is due to the assumption of $\delta_0^2g^2(x)/R^2(x)\ll 1$ being not uniformly valid at the apex for a nonvanishing $g(0)$. Apparently, this singularity is inherent to the thickness part of the solution, since in the slender-body limit, Hoffman and Platzer[8] have shown that the unsteady pressure remains regular. It can be shown that this finding also applies to flexible slender bodies. Hence, to circumvent this singularity in the formulation, the obvious choice is the body-fixed coordinate system.

Body-Fixed Coordinates

As shown in Fig. 1a, the body-fixed coordinate system requires that the x axis remain the instantaneous axis of the body, whereby each right cross section is circular and contains the r axis. Thus, the full potential Ω may be expressed as

$$\Omega(x,r,\theta,\tau)=x+\phi_0(x,r)+\delta_0e^{ik\tau}\cdot[rg'(x)+\phi_1(x,r)]\cos\theta \tag{11}$$

where the slope and curvature of the bending mode $g(x)$ and $g(x)$ itself are all of order unity. Hence, the resulting linearized equations are obtained in the same form as Eq. (4), with G_0 replaced by $G_1(g,\phi_0)$ as

$$G_1(g,\phi_0)=M_\infty^2\left[2\frac{\partial}{\partial x}\left(\phi_{0r}-r\phi_{0x}\frac{\partial}{\partial x}\right)(g'+ikg)-\left(\phi_{0r}-r\phi_{0x}\frac{\partial}{\partial x}\right)(gk^2+g'')\right]+r\frac{\partial}{\partial x}(\phi_{0x}g'')+g''(\phi_{0xx}r-\phi_{0r}) \tag{12}$$

where G_1 represents the mean flow and flexible mode interaction. This equation contains Van Dyke's[13] steady angle-of-attack equation and Hoffman and Platzer's[15] low-frequency equations as special cases. In arriving at Eq. (12), the following time derivative is applied to Eqs. (1) and (2), which relates different time scales in wind-fixed and body-fixed systems:

$$\frac{\partial}{\partial\tau}=\frac{\partial}{\partial t}-ik\delta_0e^{ikt}\left[g'r\cos\theta\frac{\partial}{\partial x}-g\cdot\left(\cos\theta\frac{\partial}{\partial r}-\frac{1}{r}\sin\theta\frac{\partial}{\partial\theta}\right)\right] \tag{13}$$

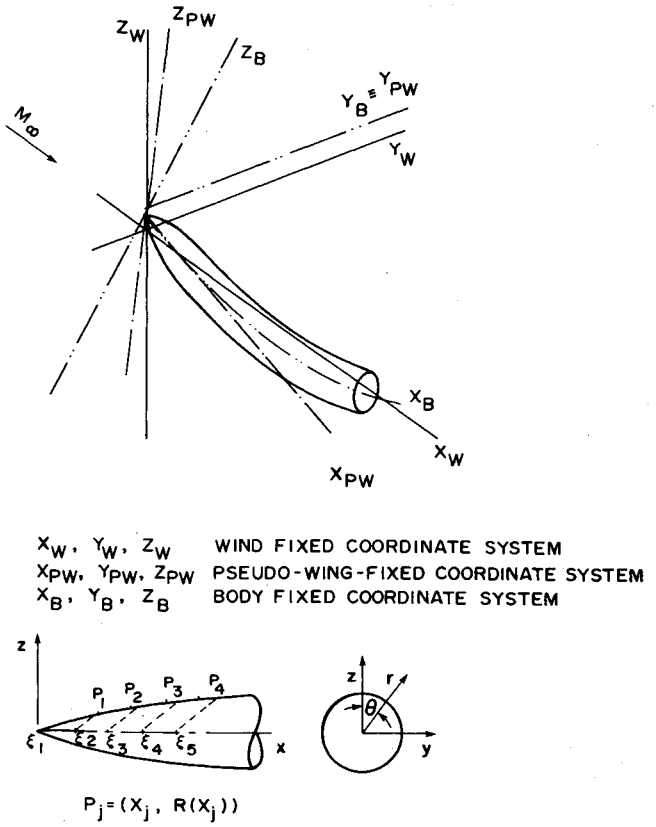

Fig. 1a Wind-fixed, body-fixed, pseudo-wind-fixed coordinate systems.

Note that Eqs. (11–13) reduce to Revell's[16] equations for rigid-body oscillation. It should be pointed out that Eq. (12) for steady flow differs from that obtained by McCanless,[17] whose resulting equation is apparently in error because the formulation was started from the linearized equation rather than the full potential equation. Now, the body surface is exactly described by $r=R(x)$, upon which the boundary condition can be expressed in the same form as Eq. (7), with B_0 replaced by B_1, i.e.,

$$B_1 = B_1(g', g'', \phi_{0x}; R, k) \tag{14}$$

Equation (7+14)[denotes Eq. (7) with the addition of Eq. (14)] reduces to Lighthill's[18] boundary condition when the second-order terms are neglected. The unsteady pressure coefficient can be expressed in the same form as Eq. (8), with J_0 replaced by J_1,

$$J_1 = J_1(g, g', g'', \phi_{0x}, \phi_{0r}; R, k) \tag{15}$$

Together with the Mach wave condition at the apex, identical to Eq. (5), Eqs. (4+12), (7+14), and (8+15) constitute the formal formulations according to the body-fixed system. To solve for Eq. (4+12), higher-order theories for slender bodies have been established by Lighthill[19] for bodies at steady angle of attack and by Revelll[16,20] for rigid-body oscillations in subsonic and supersonic flows. In terms of not-so-slender-body theory, Van Dyke[13] has shown that his "first-order" steady flow equation, $\Box\phi_1 - (1/r^2)\phi_1 = 0$, is superior in yielding better results to the linearized equation, which contains one extra term on the right-hand side, in the higher Mach number range. For bodies in low-frequency oscillations, Platzer and Sherer[10] and Tobak and Wehrend[11] adopt the first-order equation formulation and obtain stability derivatives that are in good agreement with computed results using Euler's equations. Thus, extending Van Dyke's first-order equation further into the general frequency domain amounts to neglecting the interaction terms $G_1(g,\phi_0)$ in Eq. (4+12). In this way, the linearized wave equation (4) is employed for the present formulation. Admittedly, there appears a mathematical inconsistency in this level of approximation. Nevertheless, the interaction effect due to terms in G_1 and G_2 can be recovered formally by a Green function approach proposed in the next subsection.

Pseudo-Wind-Fixed Coordinates

The present coordinate system is a hybrid one in that the x axis is not aligned with the body axis but remains rigid in motion, thus avoiding the complexity of using the curvilinear coordinates. Meanwhile, the front end of the bending mode $g(x)$ is required to attach to the origin of the x axis at all times. (See Fig. 1a.) In this way, the apex singularity can be totally removed.

Hence, the linearized equations can be obtained from Eq. (12) by letting $g(x)=x-x_0$, in the same form as Eq. (4) with G_0 replaced by $G_2(g,\phi_0)$ as

$$G_2(g,\phi_0) = M_\infty^2 \cdot \{2\phi_{0xr} + k^2[r\phi_{0x} - (x-x_0)\phi_{0r}] + 2ik(\phi_{0r} - r\phi_{0xx} + (x-x_0)\phi_{0rx})\} \tag{16}$$

where x_0 is a point chosen on the x axis so that $p(0)=0$. [See Eq. (17).] Since this equation is a degenerate from of the body-fixed equation, the justification for neglecting G_2 terms also remains valid here. The mode shape $g(x)$ expressed in this system now becomes $p(x)$, where

$$p(x) = g(x) - (x_0 - x) \tag{17}$$

The potential ϕ_1 is split into two components,

$$\phi_1(x,r) = \psi(x,r) + \lambda(x,r) \tag{18}$$

where ψ and λ represent the rigid (x-axis motion) and the flexible [$p(x)$ motion] parts of the potential, respectively. Thus, the boundary conditions, after Taylor expansion and transference to the mean surface, become, at $r=R(x)$,

$$\psi_r - R'\psi_x = -1 - ik(x - x_0 + RR') \tag{19}$$

$$\lambda_r - R'\lambda_x = -p'(x) - ikp(x) + B_2(p,\phi_0) \tag{20}$$

where

$$B_2 = B_2(p, p'; \phi_{0x}, \phi_{0xr}, \phi_{0rr}; R)$$

Notice that Eq. (20) is essentially the same as Eq. (7) of the wind-fixed system with $g(x)$ replaced by $p(x)$. The pressure coefficients C_{p1}^r and C_{p1}^f, corresponding respectively to ψ and λ, read

$$C_{p1}^r = -2S_0 \cdot \{[(1+\phi_{0x})\psi_x + \phi_{0r}\psi_r + ik\psi] + J_r\} \text{ at } r=R(x) \tag{21}$$

where

$$J_r = J_r(x - x_0, \phi_{0x}, \phi_{0r}; R, k)$$

and

$$C_{p1}^f = -2S_0 \cdot \{[(1+\phi_{0x})\lambda_x + \phi_{0r}\lambda_r + ik\lambda] + J_f\} \text{ at } r=R(x) \tag{22}$$

where

$$J_f = J_f(p, \phi_{0x}, \phi_{0r}, \phi_{0xr}, \phi_{0rr})$$

Since $p(0) = 0$ in the present system, this warrants the second-order terms such as $p(x)\phi_{0rr}$ in B_2 and J_f to be necessarily finite at the apex.

Although the apex singularity is removed in the pseudo-wind-fixed system, Eq. (22) is still not uniformly valid, since these second-order derivative terms will bear local singularities on the body where the body slope is discontinuous. In the case of the body-fixed system, however, no such singularities appear, as the unsteady pressures involve only first-order derivative terms.

Analysis

The Integral Solution

The general integral solution of Eqs. (4), (4+12), and (4+16) can be obtained by the Green function method. For $\sigma = 1$, the unsteady perturbed potential reads

$$\phi_1(x,r) = -\frac{1}{2\pi}\int_0^{x-\beta r} F(\xi)\frac{\partial}{\partial r}K(x-\xi,\beta r)\,d\xi + \phi_g \tag{23}$$

where

$$\phi_g(x,r) = \frac{1}{2\pi}\int\int_A G_n(\phi_0, g)$$

$$\times K(x-\xi,\beta r)\,d\eta\,d\xi, \qquad n = 0,1,2$$

Area A is defined in the domain downstream of the Mach wave excluding the body, i.e.,

$$R(x) \le \eta \le \xi/\beta, \quad \text{for } 0 \le \xi \le 1$$

$$0 \le \eta \le \xi/\beta, \quad \text{for } 1 \le \xi \le \infty$$

and the kernel function K is an elementary homogeneous solution of Eq. (4),[21]

$$K(x,\beta r) = e^{-i\mu x}[\cos(\nu Q)/Q] \tag{24}$$

where $Q = \sqrt{x^2 - \beta^2 r^2}$, $\mu = kM_\infty^2/\beta^2$, $\nu = kM_\infty/\beta^2$, and $F(\xi)$ is the dipole strength to be sought.

In the present analysis, we drop the inhomogeneous term ϕ_g in Eq. (23) for simplicity. But, in principle, ϕ_g can be included in the analysis since the ϕ_g integral can be evaluated if ϕ_0 is obtained from Eq. (4a) and $g(x)$ is given. In passing, we note that the equivalent nonlinear effect due to the ϕ_g term has been accounted for by Revell in his second-order theory.[16] Now, integrating Eq. (23) by parts and making use of the Mach wave condition at $x = \beta r$ yields

$$\phi_1(x,r) = -\frac{1}{2\pi}\int_x^{\beta r}\frac{\partial}{\partial x_0}[F(x-x_0)e^{-i\mu x_0}]$$

$$\times S(x_0,\beta r)\,dx_0 \tag{25}$$

where

$$S(x_0,\beta r) = \frac{\partial}{\partial r}\int_{\beta r}^{x_0}\frac{\cos(\nu Q_\tau)}{Q_\tau}d\tau$$

$$x_0 = x - \xi \quad \text{and} \quad Q_\tau = \sqrt{\tau^2 - \beta^2 r^2} \tag{26}$$

Notice that, from this point onward, x_0 is to represent the relative dipole coordinate.

Harmonic-Gradient Model

Equation (25) is to be solved based on a line-doublet panel method similar to the von Kármán-Moore procedure[22] for solving the steady mean flow. Thus, the dipole strength function is discretized into elements along the body axis from ξ_i to ξ_{i+1}, whereas the potential ϕ_1 is evaluated at the discrete field points (x_j, r_j) along the Mach wave emanating from ξ_{i+1} (see Fig. 1b),

$$\phi_1(x_j,r_j) = -\frac{1}{2\pi}\sum_{i=1}^{j}\int_{x_j-\xi_i}^{x_j-\xi_{i+1}}$$

$$\times\frac{\partial}{\partial x_0}[F_i(x_j-x_0)e^{-i\mu x_0}]S(x_0,\beta r_j)\,dx_0 \tag{27}$$

In order to achieve computational accuracy and effectiveness for handling solutions in the high-frequency range, it is important to render the doublet solution and its convective gradient uniformly valid throughout the complete frequency domain. This is to say that the doublet solution must remain spatially harmonic. In so doing, the panel size, from $R(x_j)$ to $R(x_{j+1})$, is maintained compatible to the wavenumber generated along the body in oscillation. This is the harmonic gradient (HG) concept introduced by Chen and Liu[3] for unsteady supersonic computations. Following this concept, we can similarly model the integrand of Eq. (27) as

$$\frac{\partial}{\partial x_0}[F_i(x_j-x_0)e^{-i\mu x_0}] = [a_i(x_j-x_0)+b_i]e^{-i\mu x_0} \tag{28}$$

where a_i and b_i are complex constants. This model represents a linear-harmonic doublet gradient.

Evaluation of Velocities

With the HG model of Eq. (28), Eq. (27) can be differentiated to obtain velocities ϕ_{1x} and ϕ_{1r}, i.e.,

$$\phi_{1x}(x_j,r_j) = -\frac{1}{2\pi}\sum_{i=1}^{j} a_i\int_{x_j-\xi_i}^{x_j-\xi_{i+1}} e^{-i\mu x_0}S(x_0,\beta r_j)\,dx_0 \tag{29}$$

$$\phi_{1r}(x_j,r_j) = -\frac{1}{2\pi}\sum_{i=1}^{j}\int_{x_j-\xi_i}^{x_j-\xi_{i+1}}[a_i(x_j-x_0)+b_i]e^{-i\mu x_0}$$

$$\times\frac{\partial}{\partial r_j}S(x_0,\beta r_j)\,dx_0 \tag{30}$$

Further steps are needed for evaluations of these integrands. For S in Eq. (29), applying the transform $\tau = \beta r\sqrt{1+u^2}$ to Eq. (26) results in

$$S(x_0,\beta r_j) = -\frac{x_0\cos(\nu Q_0)}{r_j Q_0} - \int_0^{Q_0/\beta r_j}$$

$$\times\lambda\beta\frac{u}{\sqrt{u^2+1}}\cdot\sin(\nu\beta r_j u)\,du \tag{31}$$

where $Q_0 = \sqrt{x_0^2 - \beta^2 r_j^2}$. Integrating Eq. (30) by parts and carrying out the differentiation with respect to r_j yields

$$\phi_{1r}(x_j,r_j) = -\frac{1}{2\pi}\sum_{i=1}^{j}\int_{x_j-\xi_i}^{x_j-\xi_{i+1}} e^{-i\mu x_0}(I_1+I_2)\,dx_0 \tag{32}$$

where

$$I_1 = -\{a_i + i\mu[a_i(x_j-x_0)+b_i]\}$$

$$\times\left[\frac{1}{\nu r_j^2}\sin(\lambda Q_0) + \beta^2\frac{\cos(\nu Q_0)}{Q_0}\right] \tag{33}$$

and

$$I_2 = [a_i(x_j - x_0) + b_i] \cdot \left[\frac{\nu x_0}{r_j^2} \sin(\nu Q_0) + \int_0^{Q_0/\beta r_j} \lambda^2 \beta^2 \frac{u^2}{\sqrt{u^2+1}} \cos(\nu \beta r_j u) \mathrm{d}u \right] \tag{34}$$

The second term in Eq. (33) is singular at the Mach cone. But this term can be recast into

$$\beta^2 \frac{\cos(\nu Q_0)}{Q_0} = -Q_0 \cos(\nu Q_0) + x_0^2 \frac{\cos(\nu Q_0)}{Q_0} \tag{35}$$

The last term of Eq. (35) and the first term of Eq. (31) can now be substituted into Eqs. (29) and (32), respectively; after integration by parts, they become numerically integrable terms.

Next, both integrals of Eqs. (31) and (34) can be approximated by applying Laschka's exponential-series substitution,[23] namely,

$$\frac{u}{\sqrt{u^2+1}} \simeq 1 - \sum_{n=1}^{N} \mathrm{d}_n e^{-ncu} \tag{36}$$

b_i can be expressed in terms of a_i by imposing the condition of equal doublet strength between adjacent elements. The value of b_i in the first element is determined by the Mach cone condition.

Finally, a_i is determined by applying Eqs. (30) and (32) to the tangency conditions Eqs. (7), (7+14), (19), and (20). The tangency condition is satified at the control points on the body at $R(x_j)$. Hence, the matrix equation is developed to evaluate a_i for given mode functions $B_j = B_n(g_j, \phi_{0j})$, $n = 0,1,2$,

$$[W_{ij}]\{a_i\} = \{B_j\} \tag{37}$$

With the unsteady pressure coefficients provided by Eqs. (8), (8+15), (21), and (22), the generalized forces are given by

$$Q_{IJ} = \frac{-1}{S_{\text{ref}}} \int_0^{2\pi} \int_0^1 C_p^{1(J)} R[g^{(I)} + RR' g'^{(I)}] \cos^2\theta \mathrm{d}\theta \mathrm{d}x \tag{38}$$

where $g^{(I)}$ is the Ith structure mode, $C_p^{1(J)}$ the pressure due to the Jth mode, and S_{ref} the reference area of the body. Here, we define S_{ref} to be the base area for the open-end bodies and the maximum cross-sectional area for the closed-end bodies.

Results and Discussion

To verify the HPP method, numerical examples are presented in terms of steady and unsteady pressures, stability derivatives, and generalized forces for various body shapes.

Figures 2–4 present the in-phase and out-of-phase pressure coefficients of a 10% thick cone at Mach number $M_\infty = 2.0$ and reduced frequency $k = 2.0$; the cone oscillates in the pitching and first and second bending modes, respectively. Free-free mode beam theory was used to determine these modes. For the rigid mode oscillation in Fig. 2, the pseudo-wind-fixed and body-fixed systems become identical; thus, only one result is presented. In general, the results of the body-fixed and the pseudo-wind-fixed systems and that of slender-body theory[5] are in good agreement. In contrast to these results, the in-phase pressures of the wind-fixed results persistently show effects of apex singualrity in all cases, as expected. Consequently, the overall pressure distributions downstream are contaminated by this singular behavior originated from the apex. It is noted that when the oscillation center x_G is placed at the apex or the mode shape $g(0)$ is zero, the apex singularity is removed and all wing-fixed results are in close agreement with the others. Also, one observes that the pressures due to flexible modes are one order higher than those of the rigid mode.

Figure 5 demonstrates that the present method can be reduced to yield correct values of steady mean velocity in the limit of zero frequency. It is seen that the present result is in good agreement with the USSAERO result as well as other theories[1,13] for a cone-cylinder body. We are of the opinion that the deviation of the USSAERO result on the aft cylinder is probably caused by an erroneous wave influence generated by the lower junction of the cone cylinder. For the low-frequency limit, Figs. 6–8 show results in damping-in-pitch moment derivatives for a parabolic ogive, an ogive cylinder, and a cone frustum. It is seen that the present HPP results are in excellent agreement with results of Platzer and Sherer's linearized method of characteristics (LMOC)[10] and Tobak and Wehrend's cone theory,[11] which are limited to the low-frequency domain. Figure 9 presents results in the high-frequency limit. Results of the present HPP code are checked against piston theory results for a very slender parabolic ogive. The thickness ratio $\tau = 0.02$ for this case is selected based on the order analysis $\tau_{M_\infty} k \leq 1$ as confined by the piston theory.[12] For $M_\infty = 1.5$, the agreement seems to be very good for two selected reduced frequencies, $k = 4.0$ and 7.5. Tables 1–3 summarize the generalized forces for a cone, parabolic ogive, and a cone cylinder with different numbers of elements according to the pseudo-wind-fixed coordinate system. Although a more accurate solution can be achieved by increasing the element numbers, as few as 40 elements seem to provide reasonably accurate generalized forces for practical flutter application. The CPU time for computing 40 panel elements usually required no more than 8 s on an IBM 3081, whereas other surface panel methods would generally require at least one order of magnitude higher.

Conclusion

Both the body-fixed and the pseudo-wind-fixed coordinate systems are found suitable for unsteady flow computations. The apex singularity of the wind-fixed coordinate system is apparently a spurious one, which requires further investigations. Thus, a harmonic potential panel (HPP) method has been developed for computations of steady and unsteady aerodynamics over elastic bodies of revolution in supersonic flow. We believe that it is the first supersonic method that can handle flexible bodies performing bending oscillations.

It has been shown that the present HPP method has the following salient features:

1) The formulation is a generalization of the harmonic gradient method for oscillating wings; it is completely general in the frequency domain.

2) It is general for axisymmetric bodies with any given body shape, allowing for slope discontinuity and any given mode shape.

3) The required number of panel elements is least affected by the given Mach number and reduced frequencies.

4) The optimized number of panels is only a fraction of those required by the surface panel method.

Therefore, we consider that the present method is computationally efficient and cost-effective. With the HPP program code developed, we await forthcoming experimental work for verification.

Most important, when the HPP code is unified with the HG code for wing planforms, it will provide the aircraft industry with an effective tool in supersonic aeroelastic applications for full aircraft or realistic missile/fin configurations. Meanwhile, further research effort in developing the HPP method is still required. For example, methods that can handle the low supersonic flow regime as well as higher Mach number effects, where nonlinearity is important, require immediate attention. Bodies with asymmetric configurations such as wave riders

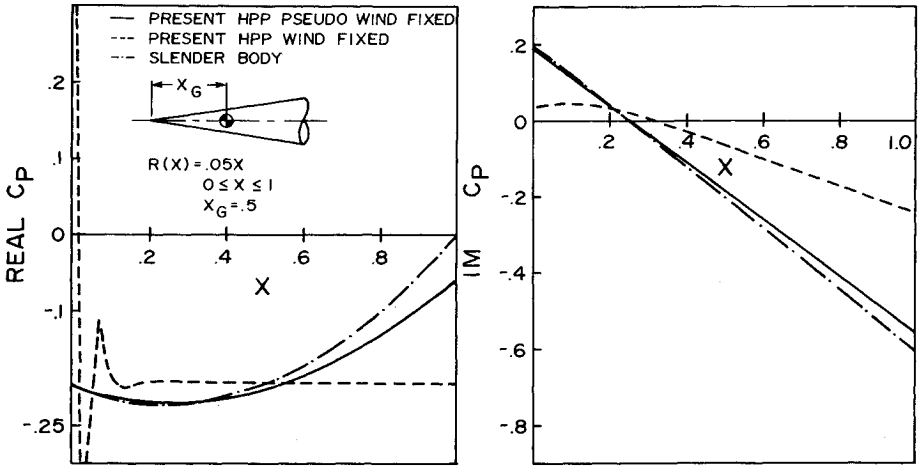

Fig. 2 In-phase and out-of-phase pressure coefficients for a cone in pitching mode at $M_\infty = 2.0$ and reduced frequency $k = 2.0$.

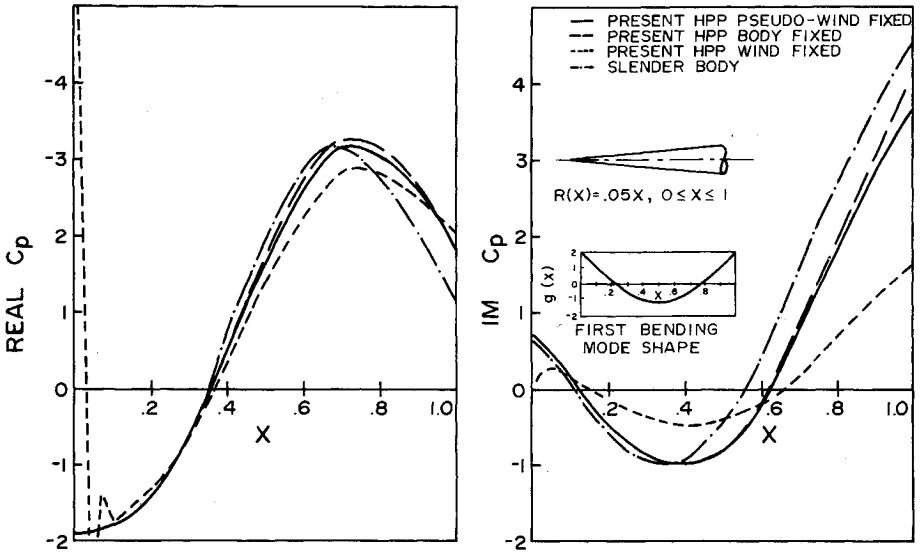

Fig. 3 In-phase and out-of-phase pressure coefficients for a cone in first bending mode at $M_\infty = 2.0$ and reduced frequency $k = 2.0$.

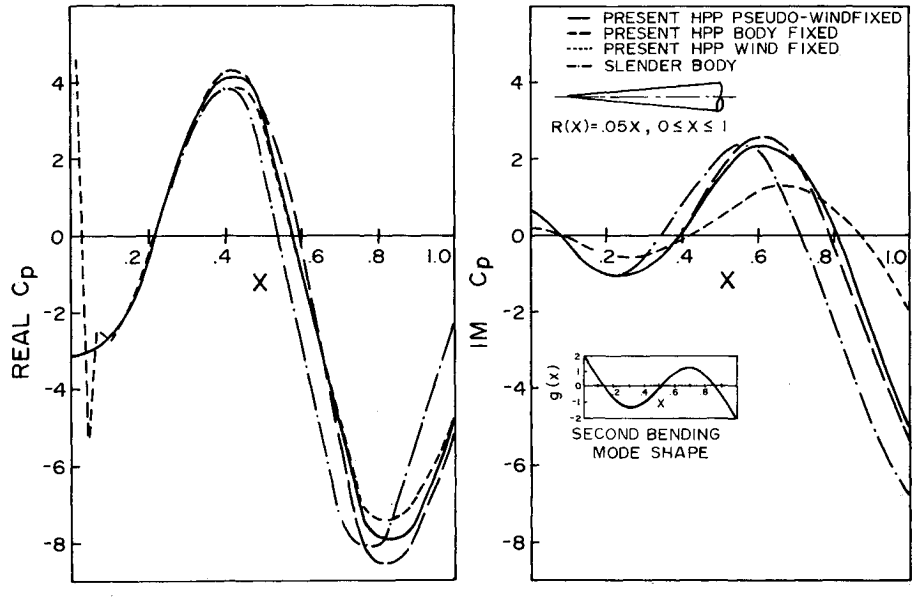

Fig. 4 In-phase and out-of-phase pressure coefficients for a cone in second bending mode at $M_\infty = 2.0$ and reduced frequency $k = 2.0$.

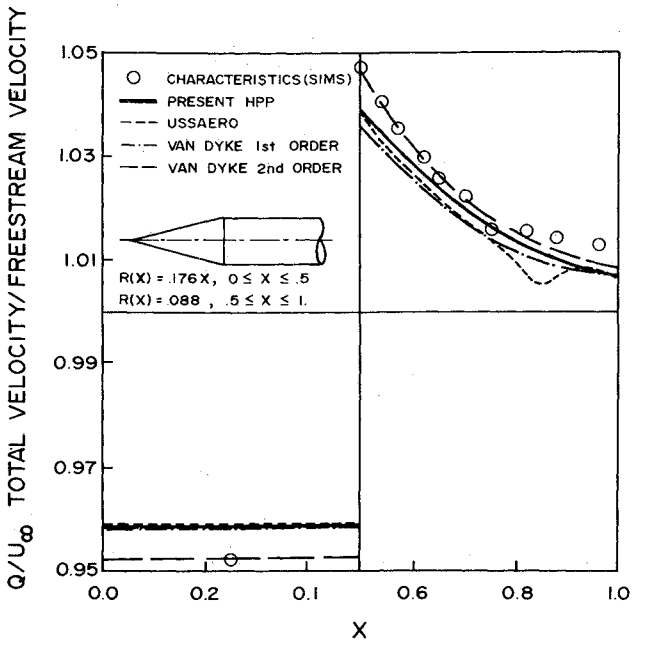

Fig. 5 Comparison of normalized velocities on a cone-cylinder surface at $M_\infty = 2.075$ and angle of attack $\alpha = 0$ deg.

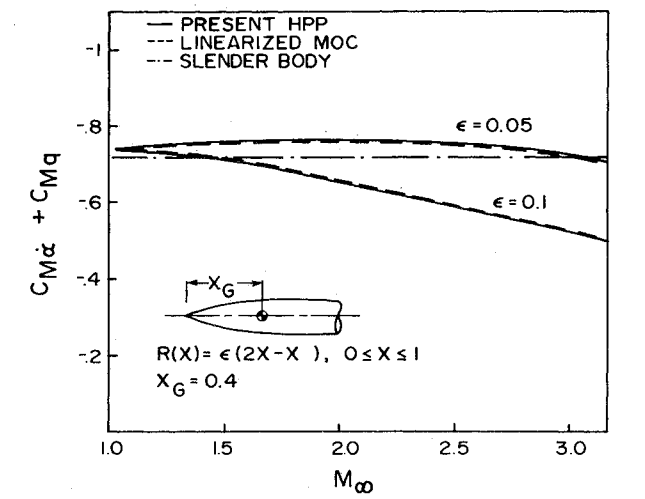

Fig. 6 Comparison of computed damping-in-pitch moment coefficients for a parabolic ogive at various Mach numbers.

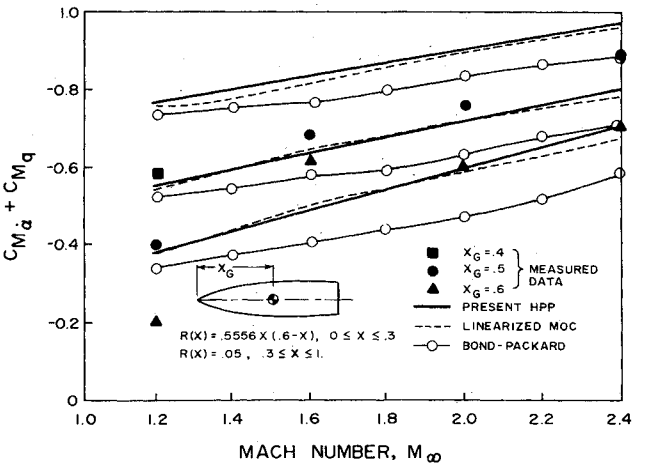

Fig. 7 Comparison of computed and measured damping-in-pitch moment coefficients for an ogive cylinder at various Mach numbers.

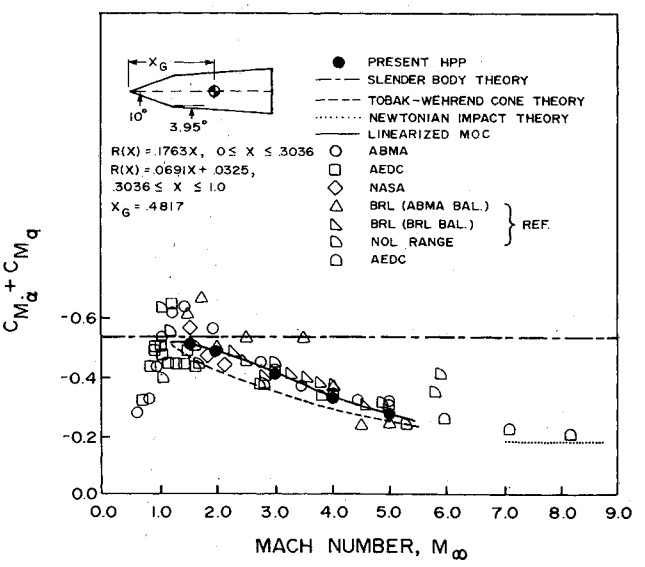

Fig. 8 Comparison of computed and measured damping-in-pitch moment coefficients for a cone frustum at various Mach numbers.

Table 1 Oscillating cone with three modes at $M_\infty = 1.5$ and $k = 2.0$. Body: $R(x) = 0.05x$, $0 \le x \le 1$; modes: 1) $g(x) = -1$; 2) $g(x) = 0.5 - x$; 3) first bending.

No.	Elements	10	20	40	60
Q_{11}	MOD	4.426	4.439	4.443	4.444
	ARG, deg	−52.54	−52.41	−52.36	−52.35
Q_{12}	MOD	3.380	3.397	3.403	3.405
	ARG, deg	−111.90	−111.61	−111.49	−111.45
Q_{13}	MOD	22.349	22.620	22.710	22.729
	ARG, deg	34.18	34.92	35.23	35.31
Q_{21}	MOD	0.901	0.890	0.887	0.887
	ARG, deg	−37.90	−37.88	−37.86	−37.86
Q_{22}	MOD	0.971	0.961	0.958	0.958
	ARG, deg	−93.03	−92.88	−92.81	−92.79
Q_{23}	MOD	8.000	7.955	7.944	7.943
	ARG, deg	49.83	50.51	50.82	50.91
Q_{31}	MOD	0.800	0.732	0.715	0.712
	ARG, deg	−175.73	−172.76	−171.93	−171.77
Q_{32}	MOD	1.438	1.339	1.315	1.310
	ARG, deg	116.55	117.75	118.09	118.16
Q_{33}	MOD	18.000	17.120	16.900	16.858
	ARG, deg	−85.96	−84.11	−83.48	−83.33
CPU time,	s	1.70	2.88	7.55	14.72

Table 2 Oscillating parabolic ogive with three modes at $M_\infty = 3.0$ and $k = 2.0$. Body: $R(x) = 0.05\ (2x - x^2)$, $0 \le x \le 1$; modes: 1) $g(x) = -1$; 2) $g(x) = -x$; 3) first bending.

No.	Elements	10	20	40	60
Q_{11}	MOD	6.224	6.215	6.210	6.208
	ARG, deg	−56.69	−56.34	−56.20	−56.17
Q_{12}	MOD	4.287	4.307	4.313	4.315
	ARG, deg	−126.66	−126.26	−126.10	−126.05
Q_{13}	MOD	23.209	23.020	22.738	22.598
	ARG, deg	5.03	5.79	6.33	6.540
Q_{21}	MOD	0.808	0.798	0.795	0.795
	ARG, deg	−12.04	−11.55	−11.42	−11.39
Q_{22}	MOD	1.054	1.045	1.042	1.041
	ARG, deg	−88.25	−87.96	−87.86	−87.83
Q_{23}	MOD	8.995	8.933	8.903	8.984
	ARG, deg	23.46	24.54	25.1	25.28
Q_{31}	MOD	1.793	1.730	1.713	1.71
	ARG, deg	−109.55	−102.82	−102.35	−102.26
Q_{32}	MOD	1.481	1.407	1.389	1.386
	ARG, deg	156.96	159.27	160.07	160.0
Q_{33}	MOD	17.695	17.34	17.24	17.216
	ARG, deg	−89.30	−87.45	−87.17	−87.20
CPU time,	s	1.70	2.77	7.46	14.62

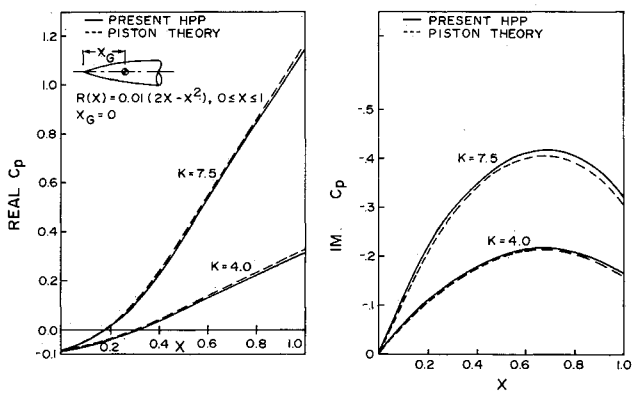

Fig. 9 In-phase and out-of-phase pressure coefficients for a parabolic ogive in pitching mode at $M_\infty = 1.5$ and reduced frequencies.

Table 3 Oscillating cone cylinder with three modes at $M_\infty = 2.0$ and $k = 2.0$. Body: $R(x) = 1.0x$, $0 \le x \le 0.5$; $R(x) = 0.05$, $0.5 \le x \le 1$, modes: 1) $g(x) = -1$; 2) $g(x) = 0.5 - x$; 3) first bending.

No.	Elements	10	20	40	60
Q_{11}	MOD	7.306	7.257	7.237	7.231
	ARG, deg	−40.77	−40.07	−39.77	−39.68
Q_{12}	MOD	5.093	5.083	5.078	5.077
	ARG, deg	−114.70	−113.86	−113.50	−113.40
Q_{13}	MOD	28.049	26.923	26.336	26.104
	ARG, deg	13.228	17.09	18.93	19.55
Q_{21}	MOD	1.378	1.363	1.358	1.358
	ARG, deg	29.06	29.48	29.59	29.61
Q_{22}	MOD	1.38	1.368	1.365	1.364
	ARG, deg	−65.04	−64.49	−64.31	−64.26
Q_{23}	MOD	10.399	10.395	10.443	10.471
	ARG, deg	43.37	47.37	48.49	48.68
Q_{31}	MOD	3.968	3.70	3.605	3.58
	ARG, deg	−91.26	−89.75	−89.22	−89.10
Q_{32}	MOD	2.886	2.728	2.675	2.662
	ARG, deg	−178.03	−175.82	−175.16	−175.02
Q_{33}	MOD	36.345	35.430	34.434	33.990
	ARG, deg	−59.38	−59.55	−60.66	−61.26
CPU time, s		1.70	2.83	7.54	14.74

and those with added fins presumably can be tackled by a generalized HPP method. Moreover, the subsonic counterpart of the supersonic HPP method can be worked out in a straightforward manner. Continuing efforts as such are currently in progress.

Acknowledgments

This work is supported by the U.S. Army Research Office, Durham, NC, contract monitors are Drs. R. E. Singleton and F. Oertel. The authors would like to thank Mr. P. C. Chen for numerous discussions and helpful suggestions on the HPP development effort. They also would like to thank Drs. W. P. Rodden, M. Landahl (MIT), M. F. Platzer (NPS), H. Ashley (Stanford), L. E. Ericsson (Lockheed Missiles & Space Co.), and M. Tobak (NASA) for valuable discussions during the course of the HPP formulation.

References

[1]Woodward, F. A., "An Improved Method for the Aerodynamic Analysis of Wing-Body-Tail Configuration in Subsonic and Supersonic Flow," NASA CR-2228, 1973.

[2]Magnus, A. E. and Epton, M. A., "PANAIR—A Computer Program for Predicting Subsonic or Supersonic Linear Potential Flows About Arbitrary Configurations Using a Higher Order Panel Method, Vol. 1: Theory Document (Version 1.0)," NASA CR-3251, 1980.

[3]Chen, P. C. and Liu, D. D., "A Harmonic Gradient Method for Unsteady Supersonic Flow Calculations," *Journal of Aircraft*, Vol. 22, May 1985, pp. 371–379.

[4]Adams, M. C. and Sears, W. R., "Slender Body Theory-Review and Extension," *Journal of the Aeronautical Sciences*, Vol. 20, Feb. 1953, pp. 85–98.

[5]Miles, J. W. and Young, D., "Generalized Missile Dynamics Analysis. III—Aerodynamics," Space Tech. Labs., Ramo-Wooldridge Corp., Rept. GM-TR-0165-00360, April 7, 1958.

[6]Lansing, D. L., "Velocity Potential and Forces on Oscillating Slender Bodies of Revolution in Supersonic Flow Expanded to the Fifth Power of the Frequency," NASA TND-1225, 1962.

[7]Bond, R. and Packard, B. B., "Unsteady Aerodynamic Forces on a Slender Body of Revolution in Supersonic Flow," NASA TND-859, May 1961.

[8]Hoffman, G. and Platzer, M. F., "On Supersonic Flow Past Oscillating Bodies of Revolution," *AIAA Journal*, Vol. 4, Feb. 1966, pp. 370–371.

[9]Labrujere, T. E., Roos, R., Erkelens, L. J. J., "The Use of Panel Methods with a View to Problems in Aircraft Dynamics," NLR MP-77009U, April 1977.

[10]Platzer, M. F. and Sherer, A. D., "Dynamic Stability Analysis of Bodies of Revolution in Supersonic Flow," *Journal of Spacecraft and Rockets*, Vol. 5, July 1968, pp. 833–837.

[11]Tobak, M. and Wehrend, W. R., "Stability Derivatives of Cones at Supersonic Speeds," NACA TN3788, Sept. 1956.

[12]Miles, J. W., *The Potential Theory of Unsteady Supersonic Flow*, Cambridge University Press, London, 1958.

[13]Van Dyke, M. D., "First and Second Order Theory of Supersonic Flow Past Bodies of Revolution," *Journal of the Aeronautical Sciences*, Vol. 18, March 1951, pp. 161–178.

[14]Platzer, M. F. and Liu, D. D., "A Linearized Characteristics Method for Supersonic Flow Past Bodies of Revolution Performing Bending Oscillations," Lockheed Missiles & Space Co., Huntsville, AL, Rept. LMSC/HREC A 784262, May 1967.

[15]Hoffman, G. H. and Platzer, M. F., "Higher Approximations for Supersonic Flow Past Slowly Oscillating Bodies of Revolution," *Acta Mechanica*, Vol. 5, 1968, pp. 143–162.

[16]Revell, J. D., "Second Order Theory for Unsteady Supersonic Flow Past Slender, Pointed Bodies of Revolution," *Journal of the Aerospace Sciences*, Vol. 27, Oct. 1960, pp. 730–740.

[17]McCanless, G. F., "Aerodynamic First-Order Method for Flexible Bodies," *Journal of Spacecraft and Rockets*, Vol. 7, Sept. 1970, pp. 1037–1042.

[18]Lighthill, M. J., "Note on the Swimming of Slender Fish," *Journal of Fluid Mechanics*, Vol. 9, 1960, pp. 305–317.

[19]Lighthill, M. J., "Supersonic Flow Past Slender Bodies of Revolution at Yaw," *Quarterly Journal of Mechanics and Applied Mathematics*, Vol. 1, March 1948, pp. 76–89.

[20]Revell, J. D., "Second Order Theory for Steady or Unsteady Subsonic Flow Past Slender Lifting Bodies of Finite Thickness," *AIAA Journal*, Vol. 7, June 1969, pp. 1070-1078.

[21]Garrick, I. E., "Nonsteady Wing Characteristics," *High Speed Aerodynamics and Jet Propulsion*, Vol. VII, Princeton University Press, Princeton, NJ, 1957, pp. 668–679.

[22]von Kármán, T. and Moore, N. B., "The Resistance of Slender Bodies," *Transactions of the ASME*, 1954, pp. 303–310.

[23]Laschka, B., "Der harmonisch Schwingende Rechteckflugel bei Ueberschallstromung," Bericht der Ernst Heinkel Flugzugbau GmbH, 1960.